

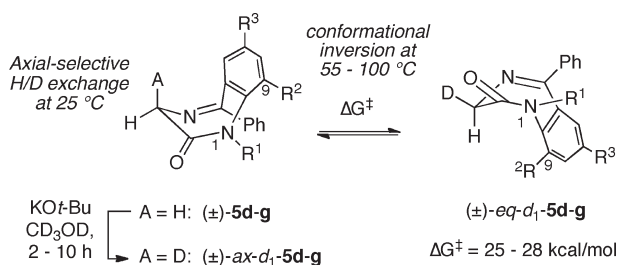
## Axial-Selective H/D Exchange of Glycine-Derived 1*H*-Benzo[*e*][1,4]diazepin-2(3*H*)-ones: Kinetic and Computational Studies of Enantiomerization

Paul R. Carlier,\* Yang-Sheng Sun, Danny C. Hsu, and Qiao-Hong Chen

Department of Chemistry, Virginia Tech, Blacksburg, Virginia 24061

pcarlier@vt.edu

Received July 11, 2010



Glycine-derived 1*H*-benzo[*e*][1,4]diazepin-2(3*H*)-ones (BZDs) **5d–g** featuring C9- and N1- substitution exhibit enantiomerization barriers too high to be measured by <sup>1</sup>H NMR coalescence experiments. To address this problem, we found that room-temperature H/D exchange of these compounds is remarkably selective, affording only the *axial-d*<sub>1</sub> isotopomers. <sup>1</sup>H NMR spectroscopy was then employed to measure the rate of conformational inversion of these *d*<sub>1</sub>-compounds at elevated temperatures. These studies reveal the highest enantiomerization barriers (up to 28 kcal/mol) ever determined for a BZD. Density functional theory calculations match the experimental enantiomerization barriers within 1.2 kcal/mol.

### Introduction

Benzo[*e*][1,4]diazepin-2(3*H*)-ones (BZDs) are well-known for their importance in medicinal chemistry.<sup>1–3</sup> We have shown that enantiopure BZDs **1b–d** undergo enantioselective deprotonation/alkylation reactions (Scheme 1).<sup>4–7</sup> The successful retentive benzylations of (*S*)-**1b–d** depicted in Scheme 1 are believed to proceed via enantiopure enolates that are chiral by virtue of the conformation of the BZD ring. Since deprotonation trigonalizes the original stereogenic center at C3, and enolate alkylation occurs with

near perfect stereoselectivity, we describe these reactions as examples of “self-regeneration of stereocenters via stereolabile axially chiral intermediates”.<sup>8–12</sup> To establish the stereochemical course of these reactions, we demonstrated by X-ray crystallography that deprotonation of (*S*)-**1d** with KHMDS at –78 °C, followed by treatment with TBS-Cl, gave enantiopure, axially chiral TBS enol (*M*)-**4d** (Scheme 2).<sup>7,13</sup>

(1) Evans, B. E.; Rittle, K. E.; Bock, M. G.; DiPardo, R. M.; Freidinger, R. M.; Whitter, W. L.; Lundell, G. F.; Veber, D. F.; Anderson, P. S.; Chang, R. S. L.; Lotti, V. J.; Cerino, D. J.; Chen, T. B.; Kling, P. J.; Kunkel, K. A.; Springer, J. P.; Hirschfield, J. *J. Med. Chem.* **1988**, *31*, 2235–2246.

(2) Ellman, J. A. *Acc. Chem. Res.* **1996**, *29*, 132–143.  
(3) Butini, S.; Gabellieri, E.; Huleatt, P. B.; Campiani, G.; Franceschini, S.; Brindisi, M.; Ros, S.; Coccone, S. S.; Fiorini, I.; Novellino, E.; Giorgi, G.; Gemma, S. *J. Org. Chem.* **2008**, *73*, 8458–8468.

(4) Carlier, P. R.; Zhao, H.; DeGuzman, J.; Lam, P. C.-H. *J. Am. Chem. Soc.* **2003**, *125*, 11482–11483.

(5) Carlier, P. R.; Lam, P. C.-H.; DeGuzman, J.; Zhao, H. *Tetrahedron: Asymmetry* **2005**, *16*, 2998–3002.

(6) Carlier, P. R.; Zhao, H.; MacQuarrie-Hunter, S. L.; DeGuzman, J. C.; Hsu, D. C. *J. Am. Chem. Soc.* **2006**, *128*, 15215–15220.

(7) Hsu, D. C.; Lam, P. C.-H.; Slebocknick, C.; Carlier, P. R. *J. Am. Chem. Soc.* **2009**, *131*, 18168–18176.

(8) Carlier, P. R.; Hsu, D. C.; Bryson, S. A. In *Stereochemical Aspects of Organolithium Compounds*; Gawley, R. E., Ed.; Topics in Stereochemistry; Siegel, J. S., Series Ed.; Verlag Helvetica Chimica Acta: Zürich, 2010; Vol. 26, p 53–92.

(9) Wolf, C. In *Dynamic Stereochemistry of Chiral Compounds: Principles and Applications*; Royal Society of Chemistry: Cambridge, UK, 2008; pp 282–289.

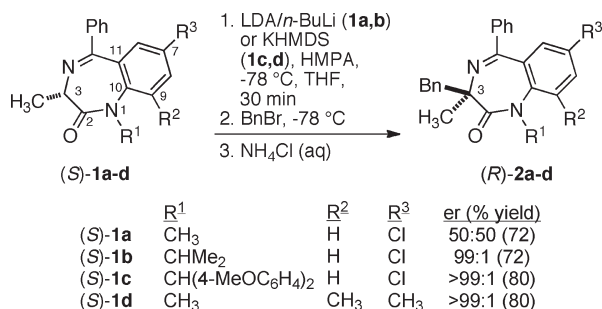
(10) Kawabata, T.; Suzuki, H.; Nagae, Y.; Fuji, K. *Angew. Chem., Int. Ed.* **2000**, *39*, 2155–2157.

(11) Kawabata, T.; Moriyama, K.; Kawakami, S.; Tsubaki, K. *J. Am. Chem. Soc.* **2008**, *130*, 4153–4157.

(12) Note that we no longer favor the term “memory of chirality,” in part because it is the configuration, not the “chirality” of the original stereogenic center that is “memorized.” We believe that the term “self-regeneration of stereocenters via stereolabile axially chiral intermediates” is more accurate and descriptive. For additional justification of this term, see refs 8 and 9.

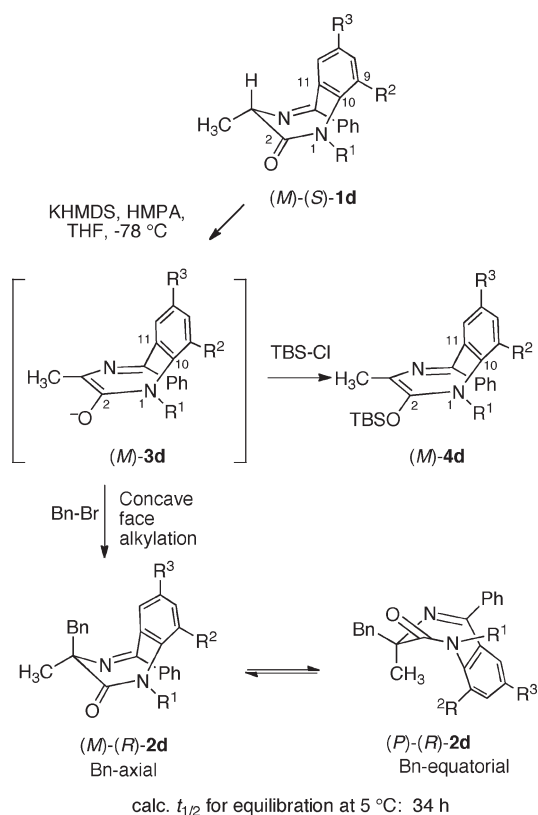
(13) The helical descriptors (*M*) and (*P*) are used to assign the sense of chirality of the ring, according to the sign of the C2N1C10C11 dihedral angle (*M* = minus, *P* = positive).

**SCHEME 1. Enantioselective Deprotonation/Benylation Reactions of (*S*)-Alanine-Derived BZDs (*S*)-1b–d<sup>a</sup>**



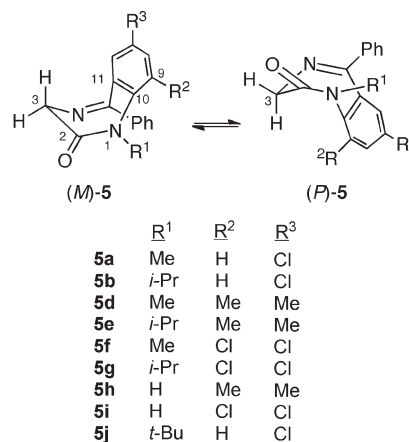
<sup>a</sup>Note that due to a Cahn–Ingold–Prelog priority switch, the configuration descriptors at C3 change following these retentive transformations.

**SCHEME 2. Stereochemical Course of Retentive Deprotonation/Benylation of (*S*)-1d**



We therefore deduce that the enolate intermediate **3d** is similarly axially chiral, and (*M*)-configured. Furthermore, <sup>1</sup>H NMR spectroscopy of the benzylation product immediately following cold work up demonstrated that **2d** is formed exclusively in the Bn-axial conformation, indicating concave face alkylation of (*M*)-**3d** (Scheme 2).<sup>7</sup> Note that on standing at room temperature, **2d** equilibrates to a mixture of Bn-axial and Bn-equatorial conformers. In the context of these results, the racemizing deprotonation/benylation of (*S*)-**1a** at –78 °C (Scheme 1) suggests that the enolate derived from **1a** completely racemizes before addition of benzyl bromide. The disparate outcomes from (*S*)-**1a** and **1d** thus point to the

**SCHEME 3. Enantiomerization and Synthesis of Glycine-Derived BZDs**



i) 1.6 equiv KH, THF, 0 °C, 1h; 10 equiv MeI, 12 h.  
 ii) 1.6 equiv KH, THF, 0 °C, 1h; 4 equiv *i*-PrOTf (**5e**) or 2 equiv *i*-PrOTf (**5g**).

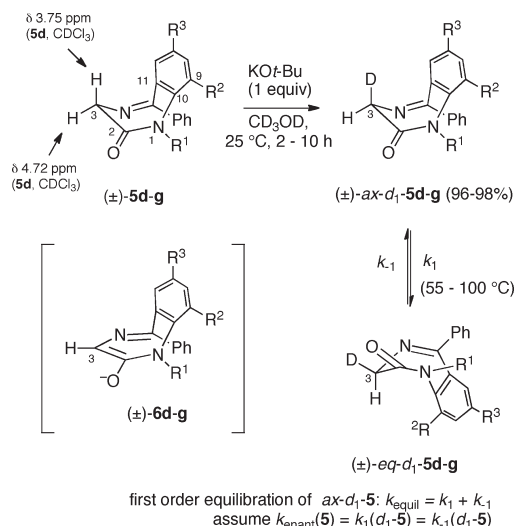
importance of steric interactions between the R<sup>1</sup> and R<sup>2</sup> group to impart a low racemization rate to the BZD enolates.<sup>4,14</sup> Consistent with this proposal, the potassium enolate derived from **1d** was experimentally determined to have an enantiomerization barrier of 19.9 ± 0.1 kcal/mol (257 K),<sup>7</sup> whereas the enantiomerization barrier of the enolate of **1a** is estimated at less than 12 kcal/mol.<sup>4,5</sup> Thus replacement of the C9–H in **1a** with methyl increased the enolate enantiomerization barrier by at least 8 kcal/mol. Consequently, deprotonation/benylation of (*S*)-**1d** occurs in greater than 99:1 er. In this paper, we describe experimental and computational studies of the effect of C9 substitution on the enantiomerization barriers of glycine-derived BZDs. We furthermore show that slow ring inversion in such compounds allows a remarkable axial-selective H/D exchange at C3.

**Results and Discussion**

Glycine-derived BZDs **5** are axially chiral and, under conditions of slow ring inversion, exhibit diastereotopic protons at C3 (Scheme 3). Since enantiomerization (ring inversion) of BZDs **5** exchanges the axial and equatorial orientation of the C3 protons (Scheme 3), <sup>1</sup>H NMR coalescence experiments can in principle be used to determine the barrier to this process. Previous application of this technique to **5a** and **5b** indicated free energies of enantiomerization ( $\Delta G^{\ddagger}_{\text{enanti}}$ ) of 18.0 ± 0.2 (391 K) and 21.3 ± 0.2 kcal/mol (437 K), respectively.<sup>14</sup> BZDs **5d–g** were then prepared from the known *N*-H analogues **5h** and **5i**,<sup>15</sup> as described in Scheme 3. Variable-temperature NMR studies of **5d** and **5f** were performed in DMSO-*d*<sub>6</sub>. However, up to the maximum temperature of the probe (453 K), coalescence of the diastereotopic C3 protons was not observed, nor was significant line broadening. Thus, enantiomerization of **5d** and

(14) Lam, P. C.-H.; Carlier, P. R. *J. Org. Chem.* **2005**, *70*, 1530–1538.

(15) Sternbach, L. H.; Fryer, R. I.; Metlesics, W.; Reeder, E.; Sach, G.; Saucy, G.; Stempel, A. *J. Org. Chem.* **1962**, *27*, 3788–3796.

**SCHEME 4. Room-Temperature Preparation of Axial- $d_1$  Isotomers of **5d–g** and Their Equilibration to the Equatorial- $d_1$  Conformers at Elevated Temperatures<sup>a</sup>**


<sup>a</sup>All compounds are racemic: (±)-**5d–g** are arbitrarily depicted in the (*M*)-conformation; (±)-*eq-d*<sub>1</sub>-**5d–g** is consequently drawn in the (*P*)-conformation.

**5g** is much slower than that of **5a**, signifying that replacement of the C9-H in **5a** with Me (**5d**) or Cl (**5f**) significantly increased the barrier to inversion.

As a possible way to determine the barrier to inversion in **5d–g** we realized that the axial- $d_1$  isotomers, if they could be prepared, would be useful for <sup>1</sup>H NMR kinetic studies. On the basis of the aforementioned studies of the stereochemistry of deprotonation and alkylation of (*S*)-**1d** (Scheme 2),<sup>7</sup> such a transformation seemed possible. As shown in Scheme 4, only the axial C3 proton of **5d–g** possesses the proper alignment with the C2–O π\* orbital to allow deprotonation. Furthermore, based on our previous studies of the stereochemistry of deprotonation/alkylation of (*S*)-**1d**,<sup>7</sup> we expected that deuteration of enolates **6d–g** should occur on the concave face only, giving *ax-d*<sub>1</sub>-**5d–g** initially. Finally, if conformational inversion of *ax-d*<sub>1</sub>-**5d–g** to *eq-d*<sub>1</sub>-**5d–g** is slow under the deprotonation conditions, then selective monodeuteration would occur.

As hoped, simple exposure of **5d–g** to KO-*t*-Bu in CD<sub>3</sub>OD gave very selective axial monodeuteration in near quantitative weight recovery (96–98%). We have previously used a similar procedure to retentively deuterate (*S*)-**1a**;<sup>5</sup> the innovation here is that axial deuteration of a racemic glycine-derived BZD is achieved, and because of slow ring inversion at room temperature, the pure *ax-d*<sub>1</sub> isotomers can be isolated. As shown in Figure 1A, **5d** has two diastereotopic protons at C3 that couple each other: axial at  $\delta$  3.75 ppm, and equatorial at  $\delta$  4.72 ppm. Upon treatment with KO-*t*-Bu in CD<sub>3</sub>OD, the signal for the axial proton disappears, and the signal for the equatorial proton becomes an apparent singlet, consistent with selective H/D exchange of the axial proton in **5d** (Figure 1B). After 4 h at 328 K, an equilibrium mixture of *ax-d*<sub>1</sub>- and *eq-d*<sub>1</sub>-**5d** is formed, as evidenced by apparent singlets of equal integration at  $\delta$  3.75 and  $\delta$  4.72 ppm (Figure 1C). The appearance of these signals as singlets, rather than as 1:1:1 triplets, reflects inability to resolve the

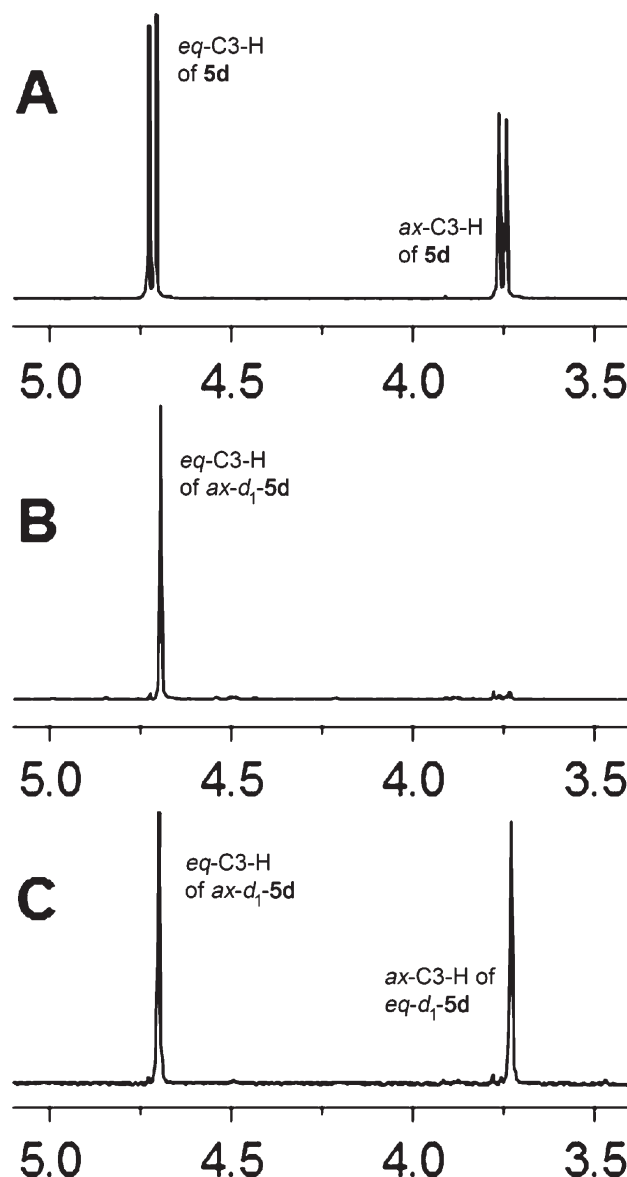


**FIGURE 1.** Room-temperature <sup>1</sup>H NMR spectra (400 MHz, CDCl<sub>3</sub>) of (A) **5d**; (B) *ax-d*<sub>1</sub>-**5d**, immediately following H/D exchange; (C) an equilibrium mixture of *ax-* and *eq-d*<sub>1</sub>-**5d**, resulting after heating *ax-d*<sub>1</sub>-**5d** for 4 h at 328 K.

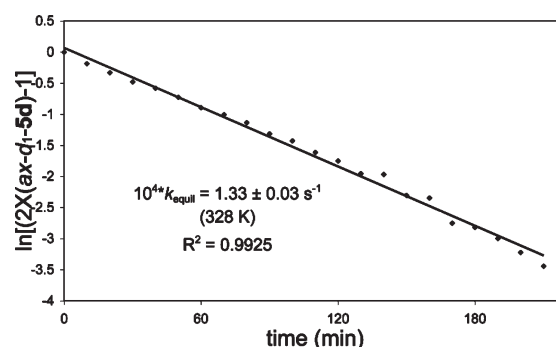


**FIGURE 2.** First-order kinetic analysis of equilibration of *ax-d*<sub>1</sub>-**5d** to the mixture of *ax-* and *eq-d*<sub>1</sub> conformers at 328 K (CDCl<sub>3</sub>). X represents mole fraction.

**TABLE 1. Measured Rates for Equilibration of *ax-d*<sub>1</sub>-Isotopomers of **5d–g**, Experimentally Derived Enantiomerization Barriers for **5d–g**, and Computed (B3LYP/6-31G\*) Enantiomerization Barriers for **5d–g****

BZD	<i>T</i> (K)	solvent	$10^4 \times k_{\text{equil}}^a$ (s <sup>-1</sup> )	exptl $\Delta G_{\text{enant}}^\ddagger(T)^b$ (kcal/mol)	B3LYP/6-31G* (PCM) $\Delta G_{\text{enant}}^\ddagger(T)^c$ (kcal/mol)
<b>5d</b>	328	CDCl <sub>3</sub>	1.33 ± 0.03	25.1 ± 0.2	26.3
<b>5e</b>	371	<i>d</i> <sub>6</sub> -DMSO	1.98 ± 0.09	28.2 ± 0.2	28.2
<b>5f</b>	328	CDCl <sub>3</sub>	0.99 ± 0.01	25.3 ± 0.2	25.1
<b>5g</b>	373	<i>d</i> <sub>6</sub> -DMSO	3.45 ± 0.12	27.9 ± 0.2	27.5

<sup>a</sup>First-order equilibration rate constants of *ax-d*<sub>1</sub>-**5d–g**, equal to  $k_1 + k_{-1}$  (Scheme 4). <sup>b</sup>For *protio-5d–g*, based on the assumption that  $k_{\text{enant}}(\mathbf{5}) = k_1(ax-d_1-5) = k_{-1}(eq-d_1-5)$ . Error estimate based on indicated uncertainties in rate and ±3 °C uncertainty in temperature. <sup>c</sup>Calculated from B3LYP/6-31G\* (PCM) electronic energies in the indicated (*protio*) solvent of the B3LYP/6-31G\* equilibrium geometries **5d–g** and enantiomerization transition structures **5d\*–g\***, incorporating free energy corrections derived from the vacuum frequencies (scaled by 0.9826) at the indicated temperature.

small two bond H–D coupling constant (expected to be 1.6 Hz)<sup>16</sup> under these conditions. However, as expected, C3 in *ax-d*<sub>1</sub>-**5d** appears as a 1:1:1 triplet in the <sup>13</sup>C NMR spectrum, due to one-bond <sup>13</sup>C–D coupling (<sup>1</sup>*J*<sub>CD</sub> = 20 Hz). Moreover, exactly analogous results were obtained when we applied the same procedure to **5e–g** (see the Supporting Information for <sup>1</sup>H NMR spectra overlays and <sup>13</sup>C NMR spectra).

If our analysis is correct, selective monodeuteration of **5a** should *not* be possible under these conditions, since unlike **5d–g**, it has a small R<sup>2</sup> substituent (H). Although H/D exchange of **5a** should initially give *ax-d*<sub>1</sub>-**5a** with high selectivity, rapid conformational inversion to *eq-d*<sub>1</sub>-**5a** will occur at room temperature (equilibration *t*<sub>1/2</sub> = 0.9 s at 25 °C, based on  $\Delta G_{\text{enant}}^\ddagger(\mathbf{5a}, 298 \text{ K}) = 18.0 \text{ kcal/mol}$ ).<sup>14</sup> Thus, axial deprotonation of *eq-d*<sub>1</sub>-**5a** should ensue, followed by deuteration, to give *d*<sub>2</sub>-**5a**. As expected, exposure of **5a** to KO-*t*-Bu in CD<sub>3</sub>OD at room temperature gave complete conversion to *d*<sub>2</sub>-**5a** within 20 min. When the experiment was repeated at 0 °C, <sup>1</sup>H NMR monitoring within 5 min showed a mixture of **5a**, *ax-d*<sub>1</sub>-**5a**, and *eq-d*<sub>1</sub>-**5a**.

The distinct <sup>1</sup>H NMR signatures of the *ax-d*<sub>1</sub>- and *eq-d*<sub>1</sub>-**5d–g** conformers and their equilibration at elevated temperatures enabled kinetic studies. As depicted in Scheme 4 for *ax-d*<sub>1</sub>-**5d**, the first-order equilibration rate constant  $k_{\text{equil}} = k_1 + k_{-1}$ . Equilibration of *ax-d*<sub>1</sub>-**5d** was observed over 4 h at 328 K, and a standard analysis for reversible first-order reaction was applied:<sup>7,17</sup> a plot of the data is shown in Figure 2. Because *ax*- and *eq-d*<sub>1</sub>-**5d** are pseudoenantiomeric isotopomers of **5d**, we assume  $k_{\text{equil}} = k_1 + k_{-1} = 2k_{\text{enant}}$ , where  $k_{\text{enant}}$  is the enantiomerization rate constant of **5d**. Therefore, we treat the equilibration of *ax-d*<sub>1</sub>-**5d** as a pseudoenantiomerization. By application of the Eyring equation<sup>18</sup> to the calculated  $k_{\text{enant}}$ , we experimentally determine  $\Delta G_{\text{enant}}^\ddagger$  (328 K) of **5d** to be 25.1 ± 0.2 kcal/mol (Table 1). Equilibration of the other *N*-Me BZD *ax-d*<sub>1</sub>-**5f** was also observed at 328 K, giving an enantiomerization barrier of 25.3 ± 0.2 kcal/mol (Table 1). The equilibration of *N-i*-Pr analogues *ax-d*<sub>1</sub>-**5e** and **5g** was very slow at 328 K but progressed rapidly at higher temperatures. Thus equilibration of these compounds was observed at 371 and 373 K, giving enantiomerization barriers of 28.2 ± 0.2 and 27.9 ± 0.2 kcal/mol, respectively (Table 1). The experimentally determined enantiomerization barriers of **5d–g** are indeed

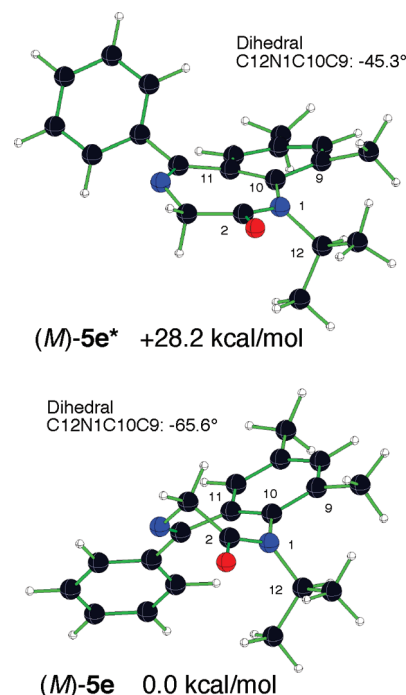


**FIGURE 3.** B3LYP/6-31G\* geometries and relative free energies (371 K) of (*M*)-**5e** (equilibrium geometry) and **5e\*** (enantiomerization transition structure). The (*M*)-enantiomers are depicted arbitrarily.

much higher than previously characterized compounds **5a**, **5b** (18.0 ± 0.2 and 21.3 ± 0.3 kcal/mol, respectively).<sup>14</sup> Comparing **5a** and **5f**, replacement of the C9-H in **5a** with Cl increased the barrier by 7.3 kcal/mol. Comparing **5b** and **5g**, replacement of the C9-H in **5b** with Cl increased the barrier by a similar amount (6.6 kcal/mol).

The nearly identical enantiomerization barriers seen for **5d** and **5f** and for **5e** and **5g** suggest that the C9-CH<sub>3</sub> and C9-Cl substituents provide a similar degree of steric hindrance to the N1 substituent in the enantiomerization transition structures. To the best of our knowledge, **5e** and **5g** have the highest enantiomerization barriers ever determined for a BZD. Gilman and co-workers demonstrated that BZD **5j** had an enantiomerization barrier  $\Delta G_{\text{enant}}^\ddagger > 24 \text{ kcal/mol}$  (variable-temperature <sup>1</sup>H NMR spectroscopy; coalescence not achieved at 473 K),<sup>19</sup> this barrier was high enough to allow preparative resolution. However, the author's observation of complete racemization of (*M*)-(-)-**5j** in solution

(16) Given that the gyromagnetic ratio of D is 6.5-fold less than that of <sup>1</sup>H, the two-bond coupling constant of the H and D at C3 in *ax-d*<sub>1</sub>-**5d** should be 6.5-fold less than the two-bond coupling constant of the axial and equatorial protons in **5d** (10.5 Hz).

(17) Connors, K. A. In *Chemical Kinetics*; VCH Publishers: New York, 1990; pp 60–61.

(18) Eyring, H. *Chem. Rev.* **1935**, *17*, 65–77.

(19) Gilman, N. W.; Rosen, P.; Earley, J. V.; Cook, C.; Todaro, L. J. *J. Am. Chem. Soc.* **1990**, *112*, 3969–3978.

TABLE 2. B3LYP/6-31G\*  $\Delta E^\ddagger_{\text{enant}}$  Values for **5a,b,d–g**, and C12N1C10C9 Dihedral Angles for the Corresponding Equilibrium Geometries and Enantiomerization Transition Structures

BZD	R <sup>1</sup>	R <sup>2</sup>	$\Delta E^\ddagger_{\text{enant}}$ <sup>a</sup> (kcal/mol)	dihedral C12N1C10C9 eq geometry <b>5a–d</b> <sup>b</sup> (deg)	dihedral C12N1C10C9 enant TS <b>5a–d</b> <sup>c</sup> (deg)
<b>5a</b>	Me	H	17.3	33.6	6.0
<b>5b</b>	<i>i</i> -Pr	H	20.0	43.5	18.3
<b>5f</b>	Me	Cl	23.9	53.6	30.5
<b>5d</b>	Me	Me	24.2	54.6	32.0
<b>5g</b>	<i>i</i> -Pr	Cl	26.5	63.6	43.2
<b>5e</b>	<i>i</i> -Pr	Me	26.9	65.6	45.3

<sup>a</sup>Energies are ZPVE-corrected to calculate  $\Delta E^\ddagger_{\text{enant}}$ . <sup>b</sup>Absolute values of dihedral angles for **5a,b,d–g**: note the dihedral angles are < 0 for the (*M*)-enantiomers. <sup>c</sup>Absolute values of dihedral angles for **5a\*,b\*,d\*–g\***: note the dihedral angles are < 0 for the (*M*)-enantiomers.

within 3 days at room temperature also suggests a barrier less than 24.5 kcal/mol.<sup>20</sup>

We have previously been successful in matching experimental enantiomerization barriers of benzodiazepines<sup>14</sup> and benzodiazepine enolates<sup>7</sup> with calculated values of  $\Delta G^\ddagger_{\text{enant}}$  derived from density functional calculations. We therefore located the minimum energy equilibrium geometries of **5d–g** and the corresponding enantiomerization transition structures **5d\*–g\*** at B3LYP/6-31G\*.<sup>21</sup> Representative structures (*M*)-**5e** and (*M*)-**5e\*** are depicted in Figure 3.

As noted in our previous studies, BZD equilibrium geometries adopt a boat conformation. In contrast, BZD enantiomerization transition structures are considerably but not completely flattened and, therefore, exist as a pair of (*M*)- and (*P*)-enantiomers.<sup>14</sup> To calculate  $\Delta G^\ddagger_{\text{enant}}$  from these structures, we applied free energy and polarized continuum model (PCM) solvent corrections at the experimental temperature and solvent (CHCl<sub>3</sub> or DMSO). As can be seen in Table 1, excellent agreement is seen between experiment and theory for **5d–g**, with the largest deviation being 1.2 kcal/mol. Since the equilibrium geometries and enantiomerization transition structures of **5a** and **5b** had not been calculated previously, we also located these structures, and again applied the appropriate free energy and PCM corrections. The enantiomerization free energies obtained for **5a** and **5b** (17.5 and 21.5 kcal/mol) also match experimental values very well (18.0 ± 0.2 and 21.3 ± 0.3 kcal/mol, respectively).<sup>14</sup>

To gain further insight into the role that the R<sup>1</sup> and R<sup>2</sup> substituents play in determining the experimental free energy of activation  $\Delta G^\ddagger_{\text{enant}}$ , we inspected the B3LYP/6-31G\*

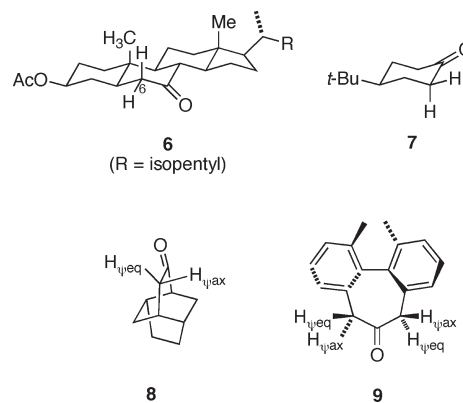


FIGURE 4. Selected cyclic ketones examined in the literature for axial-selective deprotonation.

equilibrium geometries and enantiomerization transition structures of **5a,b,d–g** in detail: an extensive tabulation of bond angles and dihedral angles can be found in the Supporting Information. From these studies, we noted that the absolute value of the C12N1C10C9 dihedral (see Figure 2), which reflects torsional interactions between the N1 substituent and C9, is correlated well to the calculated  $\Delta E^\ddagger_{\text{enant}}$  values<sup>22</sup> (Table 2). Specifically, as  $\Delta E^\ddagger_{\text{enant}}$  increases from 17.3 kcal/mol (**5a**) to 26.9 kcal/mol (**5e**), there is a steady increase in the C12N1C10C9 dihedral angle, both in the equilibrium geometries and in the enantiomerization transition structures. Comparison of **5a** and **5b**, **5f** and **5g**, **5d** and **5e** shows that as the size of the R<sup>1</sup> substituent increases, so does the C12N1C10C9 dihedral (both equilibrium geometry and enantiomerization transition structure) and the  $\Delta E^\ddagger_{\text{enant}}$  value. A similar trend is seen for increasing the size of the R<sup>2</sup> substituent (cf. **5a** vs **5f,d**; **5b** vs **5g,e**). These trends in dihedral angles suggest the need to relieve steric interactions between R<sup>1</sup> and R<sup>2</sup> as these substituents increase in size. Since in every case the dihedral angle *decreases* on proceeding from an equilibrium geometry to the corresponding enantiomerization transition structure (e.g., 33.6° in **5a** to 6.0° in **5a\***), steric interaction between the R<sup>1</sup> and R<sup>2</sup> substituents must increase during enantiomerization. Thus the energetic consequences of increasing the size of the R<sup>1</sup> and/or R<sup>2</sup> substituents are greater for the enantiomerization transition structures than for the equilibrium geometries, leading to the 9.6 kcal/mol increase in  $\Delta E^\ddagger_{\text{enant}}$  seen from **5a** to **5e**.

In closing this section, we wish to provide further context for the very high axial selectivity seen in both the deprotonation of **5d–g** and in the deuteration of the corresponding enolates. The term “stereoelectronic control”, as first introduced by Corey and Sreen in 1956,<sup>23</sup> concerned deprotonation of carbonyl compounds, and protonation of the corresponding enols or enolates. As a class, cyclohexanone derivatives might be expected to show high deprotonation stereoselectivity, due to chair conformational preference and consequent differentiation of axial and equatorial  $\alpha$ -protons relative to the C=O  $\pi^*$  orbital. However to date, axial selectivities for deprotonation of such compounds

(20) Calculation of the  $k_{\text{rac}}$  for **5j** from  $\Delta G^\ddagger_{\text{enant}} = 24.5$  kcal/mol (298 K) and assumption of first-order racemization would predict < 3% ee after 72 h.

(21) Gaussian 03, Revision B.05: Frisch, M. J.; Trucks, G. W.; Schlegel, H. B.; Scuseria, G. E.; Robb, M. A.; Cheeseman, J. R.; Montgomery, J. A., Jr.; Vreven, T.; Kudin, K. N.; Burant, J. C.; Millam, J. M.; Iyengar, S. S.; Tomasi, J.; Barone, V.; Mennucci, B.; Cossi, M.; Scalmani, G.; Rega, N.; Petersson, G. A.; Nakatsuji, H.; Hada, M.; Ehara, M.; Toyota, K.; Fukuda, R.; Hasegawa, J.; Ishida, M.; Nakajima, T.; Honda, Y.; Kitao, O.; Nakai, H.; Klene, M.; Li, X.; Knox, J. E.; Hratchian, H. P.; Cross, J. B.; Adamo, C.; Jaramillo, J.; Gomperts, R.; Stratmann, R. E.; Yazyev, O.; Austin, A. J.; Cammi, R.; Pomelli, C.; Ochterski, J. W.; Ayala, P. Y.; Morokuma, K.; Voth, G. A.; Salvador, P.; Dannenberg, J. J.; Zakrzewski, V. G.; Dapprich, S.; Daniels, A. D.; Strain, M. C.; Farkas, O.; Malick, D. K.; Rabuck, A. D.; Raghavachari, K.; Foresman, J. B.; Ortiz, J. V.; Cui, Q.; Baboul, A. G.; Clifford, S.; Cioslowski, J.; Stefanov, B. B.; Liu, G.; Liashenko, A.; Piskorz, P.; Komaromi, I.; Martin, R. L.; Fox, D. J.; Keith, T.; M. A. Al-Laham, Peng, C. Y.; Nanayakkara, A.; Challacombe, M.; Gill, P. M. W.; Johnson, B.; Chen, W.; Wong, M. W.; Gonzalez, C.; Pople, J. A. Gaussian, Inc., Pittsburgh, PA, 2003.

(22) We chose to compare  $\Delta E^\ddagger_{\text{enant}}$  values, to avoid any possible bias due to differences in calculated  $T\Delta S^\ddagger$  terms. However, the same trend is seen in calculated  $\Delta G^\ddagger_{\text{enant}}(T)$  values, with and without PCM corrections.

(23) Corey, E. J.; Sreen, R. A. *J. Am. Chem. Soc.* **1956**, *78*, 6269–6278.

(and protonation of their enolates) have been very low. Corey reported selectivities less than 2-fold for axial vs equatorial deprotonation of 3- $\beta$ -acetoxycholestan-7-one **6** at C6; selectivities for protonation of the corresponding enols were also less than 2-fold (Figure 4).<sup>23</sup> Simple 4-*tert*-butylcyclohexanone **7** is reported to show only 5.5-fold selectivity for deprotonation of the axial proton relative to the equatorial proton,<sup>24</sup> and a number of other cyclohexanone derivatives show similarly low selectivity.<sup>25</sup> One important counter-example is provided by twistan-4-one **8**, which is reported to show a 290-fold preference for deprotonation of pseudoaxial proton H <sub>$\psi$ ax</sub> relative to pseudoequatorial proton H <sub>$\psi$ eq</sub>.<sup>26</sup> The authors attribute the selectivity to better orbital overlap of the C–H <sub>$\psi$ ax</sub> bond with the carbonyl group. Finally, C<sub>2</sub>-symmetric cycloheptanone **9** was shown to exhibit a 73-fold preference for H/D exchange of pseudoaxial proton H <sub>$\psi$ ax</sub> relative to pseudoequatorial proton H <sub>$\psi$ eq</sub>, a result again interpreted in terms of better orbital overlap during deprotonation.<sup>27</sup> It should be noted that for both **8** and **9**, selectivities in the enolate deuteration step must also be high. On the basis of the similar structural features of **5d–g** and **9**, it is tempting to speculate that slow rotation of the biaryl bond in the enolate derived from **9** is also critical to achieving high facial selectivity in the deuteration step.

## Conclusion

In conclusion, we demonstrated that the C3 H/D exchange of **5d–g** at room temperature is remarkably selective, affording the *ax-d*<sub>1</sub> isotopomers exclusively. In contrast, when **5a** was subjected to the same conditions, it afforded *d*<sub>2</sub>-**5a** within 20 min at room temperature. The selectivity seen for **5d–g** is attributed to three factors: exclusive axial deprotonation, exclusive concave-face deuteration, and slow conformational inversion of *ax-d*<sub>1</sub>-**5d–g** to *eq-d*<sub>1</sub>-**5d–g** under the deprotonation conditions. In the case of **5a**, the presence of a small R<sup>2</sup> substituent (H) allows fast conformational inversion of *ax-d*<sub>1</sub>-**5a** to *eq-d*<sub>1</sub>-**5a** under the deprotonation conditions, resulting in a second deprotonation and deuteration.

The *ax-d*<sub>1</sub>-isotopomers of **5d–g** were then used to experimentally determine the enantiomerization barriers of glycine-derived BZDs **5d–g** by observing their equilibration to a mixture of the *ax*- and *eq-d*<sub>1</sub> conformers by <sup>1</sup>H NMR spectroscopy at elevated temperatures. These studies revealed enantiomerization barriers of 25–28 kcal/mol. Density functional theory calculations matched these experimental barriers to within 1.2 kcal/mol, and demonstrated a correlation between the enantiomerization barrier and the C12N1C10C9 dihedral angle in both the equilibrium geometries and enantiomerization transition structures. These studies and the insights gained herein should prove useful for designing other systems in which to achieve enantioselective reaction of stereolabile intermediates.

(24) Trimitsis, G. B.; Van Dam, E. M. *J. Chem. Soc., Chem. Commun.* **1974**, 610–611.

(25) Pollack, R. M. *Tetrahedron* **1989**, *45*, 4913–4938.

(26) Fraser, R. R.; Champagne, P. J. *J. Am. Chem. Soc.* **1978**, *78*, 657–658.

(27) Fraser, R. R.; Champagne, P. J. *Can. J. Chem.-Rev. Can. Chim.* **1976**, *54*, 3809–3811.

(28) Beard, C. D.; Baum, K.; Grakauskas, V. J. *Org. Chem.* **1973**, *38*, 3673–3677.

## Experimental Section

**General Procedure A: N1-Alkylation of Gly-Derived N-H 1,4-Benzodiazepin-2-ones.** The Gly-derived N-H 1,4-benzodiazepin-2-one **5h** or **5i** (0.60 g, 2.2 mmol, 1 equiv) dissolved in anhydrous THF (15 mL) was added to potassium hydride or sodium hydride (1.6 equiv) at 0 °C under nitrogen. The resulting solution was stirred at 0 °C for 30 min. The alkylating agent (MeI, *i*-PrOTs, or *i*-PrOTf<sup>28</sup>) was added dropwise to the solution, the reaction mixture was stirred for 6 h at room temperature, quenched by the addition of satd NH<sub>4</sub>Cl (aq), and extracted with CH<sub>2</sub>Cl<sub>2</sub> (3 × 30 mL). The combined organic extracts were dried over Na<sub>2</sub>SO<sub>4</sub>, filtered, and concentrated. The crude product was purified by flash column chromatography on silica gel (2:1 EtOAc/hexanes).

**General Procedure B: Axial-Selective H/D Exchange of Gly-Derived 1,4-Benzodiazepin-2-ones.** The *N*-alkyl-Gly-derived BZD **5d–g** (20–30 mg, 1 equiv) was dissolved in CD<sub>3</sub>OD (2 mL), and KO-*t*-Bu (1 equiv) was added; note that dissolution of **5g** required addition of a few drops of CDCl<sub>3</sub>. After dissolution, the mixture was transferred to an NMR tube, and the reaction was monitored by <sup>1</sup>H NMR for 2–10 h at room temperature to ensure complete H/D exchange of the axial C3-proton. The reaction was quenched by addition of satd NH<sub>4</sub>Cl (aq, 0.25 mL), and the CD<sub>3</sub>OD was removed in vacuo. The aqueous suspension was extracted with CH<sub>2</sub>Cl<sub>2</sub> (3 × 5 mL). The combined organic extracts were dried over anhydrous Na<sub>2</sub>SO<sub>4</sub>, filtered, and concentrated. The monodeuterated products were obtained in 96–98% weight recovery and needed no further purification. As discussed in this paper and below, the products isolated in this way featured exclusive axial deuteration. Furthermore, <sup>1</sup>H NMR integrals and HRMS analysis were consistent with < 10% *d*<sub>2</sub>-byproduct. No attempts were made to more accurately quantitate this potential contaminant, since it would not interfere with our <sup>1</sup>H NMR kinetic studies. However, according to our current mechanistic understanding, *d*<sub>2</sub>-byproduct would accrue only from deprotonation/deuteration of *eq-d*<sub>1</sub>-**5d–g**. Based on our measured  $\Delta G^{\ddagger}_{\text{enantiomer}}$  values (Table 1 of manuscript), we estimate that *ax-d*<sub>1</sub>-**5d** and **5f** would equilibrate to a 95:5 mixture of *ax-d*<sub>1</sub> and *eq-d*<sub>1</sub> conformers over 6 h at room temperature. For *N*-*i*-Pr analogues **5e** and **5g**, we estimate that the *ax-d*<sub>1</sub> conformers would still be >99% populated after 6 h at room temperature. These calculations are consistent with our estimation of < 10% *d*<sub>2</sub>-byproduct in *ax-d*<sub>1</sub>-**5d–g**.

**1,7,9-Trimethyl-5-phenyl-1H-benzo[e][1,4]diazepin-2(3H)-one (5d).** The following were used in general procedure A above: **5h** (0.30 g, 1.1 mmol, 1.0 equiv), KH (0.24 g, 1.8 mmol, 1.6 equiv, 30% suspension in mineral oil), methyl iodide (2.1 mL, 33 mmol, 30 equiv). Purification with flash column chromatography on silica gel (1:2 EtOAc/hexanes) provided **5d** (0.29 g, 91%) as pale yellow solid; mp 102–103 °C; <sup>1</sup>H NMR (CDCl<sub>3</sub>, 500 MHz):  $\delta$  7.67 (br d, *J* = 7.5 Hz, 2H), 7.45 (br t, *J* = 7.5 Hz, 1H), 7.39 (br d, *J* = 7.5 Hz, 2H), 7.20 (br s, 1H), 6.90 (br s, 1H), 4.72 (d, *J* = 10.5, 1H), 3.75 (d, *J* = 10.5 Hz, 1H), 3.18 (s, 3H), 2.36 (s, 3H), 2.28 (s, 3H); <sup>13</sup>C NMR (CDCl<sub>3</sub>, 125 MHz)  $\delta$  170.5, 170.2, 140.8, 139.1, 135.3, 134.9, 132.7, 130.3, 129.5, 128.3, 127.8, 56.9, 36.6, 20.9, 19.8; HRMS (EI) calcd for C<sub>18</sub>H<sub>18</sub>N<sub>2</sub>O (M<sup>+</sup>) 278.141913, found 278.143077 (–4.2 ppm, –1.2 mDa).

**Axial 3-Deuterio-1,7,9-trimethyl-5-phenyl-1H-benzo[e][1,4]diazepin-2(3H)-one (ax-d<sub>1</sub>-5d).** General procedure B was applied twice to **5d** on a 20–30 mg scale. H/D exchange was complete within 2 h, and the desired axially deuterated product *ax-d*<sub>1</sub>-**5d** was obtained in an average 97% weight recovery: <sup>1</sup>H NMR (CDCl<sub>3</sub>, 500 MHz):  $\delta$  7.67 (dt, *J* = 7.2, 1.6 Hz, 2H), 7.45 (tt, *J* = 7.2, 2.4 Hz, 1H), 7.39 (tt, *J* = 7.2, 1.6 Hz, 2H), 7.20 (br s, 1H), 6.90 (br s, 1H), 4.69 (s, 1H), 3.18 (s, 3H), 2.36 (s, 3H), 2.28 (s, 3H); <sup>13</sup>C NMR (CDCl<sub>3</sub>, 125 MHz)  $\delta$  170.5, 170.2, 140.8, 139.1, 135.3, 134.8, 132.8, 130.34, 130.32, 129.5, 128.3, 127.8, 56.6 (t,

$^1J_{\text{CD}} = 20.0$  Hz), 36.6, 20.8, 19.8. Equilibrium mixture of *ax-d*<sub>1</sub>-**5d** and *eq-d*<sub>1</sub>-**5d**:  $^1\text{H NMR}$  ( $\text{CDCl}_3$ , 500 MHz)  $\delta$  7.66 (dt,  $J = 7.0$ , 1.6 Hz, 2H), 7.44 (tt,  $J = 7.2$ , 2.4 Hz, 1H), 7.39 (tt,  $J = 7.0$ , 1.6 Hz, 2H), 7.19 (br s, 1H), 6.90 (br s, 1H), 4.69 (s, 0.5 H, equatorial), 3.73 (s, 0.5 H, axial), 3.10 (s, 3H), 2.36 (s, 3H), 2.28 (s, 3H); HRMS(EI) calcd for  $\text{C}_{18}\text{H}_{17}\text{N}_2\text{O}$  ( $\text{M}^+$ ) 279.1482, found 279.1493 (−4.09 ppm, −1.2 mDa).

**1-Isopropyl-7,9-dimethyl-5-phenyl-1*H*-benzo[e][1,4]diazepin-2(3*H*)-one (5e).** The following were used in general procedure A above: 5 h (0.30 g, 1.1 mmol, 1 equiv), KH (0.24 g, 1.8 mmol, 1.6 equiv, 30% suspension in mineral oil), isopropyl tosylate (0.94 g, 4.4 mmol, 4 equiv). Purification with flash column chromatography on silica gel (1:2 EtOAc/hexanes) provided **5e** (0.15 g, 44%) as pale yellow solid: mp 160–162 °C;  $^1\text{H NMR}$  ( $\text{CDCl}_3$ , 500 MHz)  $\delta$  7.71 (br d,  $J = 7.2$  Hz, 2H), 7.46 (tt,  $J = 7.2$ , 1.4 Hz, 1H), 7.41 (br t,  $J = 7.2$  Hz, 2H), 7.21 (br s, 1H), 6.86 (br s, 1H), 4.57 (d,  $J = 9.8$  Hz, 1H), 3.65 (d,  $J = 9.8$  Hz, 1H), 3.46 (hept,  $J = 6.8$  Hz, 1H), 2.41 (s, 3H), 2.28 (s, 3H), 1.73 (d,  $J = 6.8$  Hz, 3H), 1.13 (d,  $J = 6.8$  Hz, 3H);  $^1\text{H NMR}$  ( $\text{DMSO-}d_6$ , 500 MHz)  $\delta$  7.65 (br d,  $J = 7.0$  Hz, 2H), 7.52 (tt,  $J = 7.0$ , 2.4 Hz, 1H), 7.47 (tt,  $J = 7.0$ , 1.6 Hz, 2H), 7.36 (br s, 1H), 6.82 (br s, 1H), 4.33 (d,  $J = 9.8$  Hz, 1H), 3.56 (d,  $J = 9.8$  Hz, 1H), 3.45 (hept,  $J = 6.8$  Hz, 1H), 2.39 (s, 3H), 2.25 (s, 3H), 1.64 (d,  $J = 6.8$  Hz, 3H), 0.98 (d,  $J = 6.8$  Hz, 3H);  $^{13}\text{C NMR}$  ( $\text{CDCl}_3$ , 125 MHz)  $\delta$  170.1, 169.6, 141.3, 139.0, 135.5, 134.7, 133.9, 131.3, 130.3, 129.4, 128.4, 127.4, 58.8, 56.5, 21.5, 20.8, 19.9, 18.4; HRMS (EI) calcd for  $\text{C}_{20}\text{H}_{22}\text{N}_2\text{O}$  ( $\text{M}^+$ ) 306.1732, found 306.174 (−2.45 ppm, −1.2 mDa).

**Axial 3-Deuterio-1-isopropyl-7,9-dimethyl-5-phenyl-1*H*-benzo[e][1,4]diazepin-2(3*H*)-one (*ax-d*<sub>1</sub>-**5e**).** General procedure B was applied twice to **5e** on a 20–30 mg scale. H/D exchange required 10 h and gave the desired axially deuterated product in an average 96% weight recovery:  $^1\text{H NMR}$  ( $\text{CDCl}_3$ , 500 MHz)  $\delta$  7.71 (dt,  $J = 7.2$ , 1.6 Hz, 2H), 7.46 (tt,  $J = 7.2$ , 1.6 Hz, 1H), 7.41 (tt,  $J = 7.2$ , 1.6 Hz, 2H), 7.21 (br s, 1H), 6.87 (br s, 1H), 4.54 (s, 1H), 3.46 (hept,  $J = 6.8$  Hz, 1H), 2.41 (s, 3H), 2.27 (s, 3H), 1.73 (d,  $J = 6.8$  Hz, 3H), 1.13 (d,  $J = 6.8$  Hz, 3H);  $^{13}\text{C NMR}$  ( $\text{CDCl}_3$ , 125 MHz) 170.1, 169.6, 141.3, 139.0, 135.4, 134.7, 133.9, 131.3, 130.3, 129.4, 128.4, 127.4, 58.6 (t,  $^1J_{\text{CD}} = 20$  Hz), 56.5, 21.5, 20.8, 19.9, 18.4;  $^1\text{H NMR}$  ( $\text{DMSO-}d_6$ , 500 MHz)  $\delta$  7.66 (br d,  $J = 6.9$  Hz, 2H), 7.53 (br t,  $J = 6.9$  Hz, 1H), 7.48 (br t,  $J = 6.9$  Hz, 2H), 7.35 (br s, 1H), 6.83 (br s, 1H), 4.31 (s, 1H), 3.46 (hept,  $J = 6.8$  Hz, 1H), 2.40 (s, 3H), 2.26 (s, 3H), 1.65 (d,  $J = 6.8$  Hz, 3H), 0.99 (d,  $J = 6.8$  Hz, 3H). Equilibrium mixture of *ax-d*<sub>1</sub>-**5e** and *eq-d*<sub>1</sub>-**5e**:  $^1\text{H NMR}$  ( $\text{DMSO-}d_6$ , 500 MHz)  $\delta$  7.64 (br d,  $J = 7.9$  Hz, 2H), 7.52 (br t,  $J = 7.9$  Hz, 1H), 7.47 (br t,  $J = 7.9$  Hz, 2H), 7.35 (br s, 1H), 6.82 (br s, 1H), 4.31 (s, 0.5 H, equatorial), 3.54 (s, 0.5 H, axial), 3.45 (hept,  $J = 6.8$  Hz, 1H), 2.39 (s, 3H), 2.25 (s, 3H), 1.64 (d,  $J = 6.8$  Hz, 3H), 0.98 (d,  $J = 6.8$  Hz, 3H); HRMS (EI) calcd for  $\text{C}_{20}\text{H}_{21}\text{N}_2\text{O}$  ( $\text{M}^+$ ) 307.1795, found 307.1803 (−2.71 ppm, −1.2 mDa).

**3,3-Dideuterio-7-chloro-1-methyl-5-phenyl-1*H*-benzo[e][1,4]diazepin-2(3*H*)-one (*d*<sub>2</sub>-**5a**).** General procedure B was applied twice on a 10–15 mg scale to **5a**,<sup>15</sup> giving *d*<sub>2</sub>-**5a** in an average 97% weight recovery. When the exchange was performed at room temperature, complete conversion to *d*<sub>2</sub>-**5a** was observed within 20 min. When the  $\text{CD}_3\text{OD}$  was precooled to 0 °C and the reaction mixture was kept at 0 °C for 5 min, the  $^1\text{H NMR}$  spectrum indicated a mixture of starting material, *ax-d*<sub>1</sub>-**5a**, and *eq-d*<sub>1</sub>-**5a**. The reaction mixture was then warmed to room temperature and monitored by  $^1\text{H NMR}$  spectroscopy. It was found that H/D exchange of the both C3-protons was complete after 40 min of total reaction time:  $^1\text{H NMR}$  ( $\text{CDCl}_3$ , 500 MHz)

$\delta$  7.59 (dt,  $J = 7.2$ , 1.7 Hz, 2H), 7.51 (dd,  $J = 7.2$ , 2.5 Hz, 1H), 7.47 (dt,  $J = 7.6$ , 2.5 Hz, 1H), 7.41 (tt,  $J = 7.2$ , 1.6 Hz, 2H), 7.29 (d,  $J = 7.2$  Hz, 1H), 7.28 (d,  $J = 2.5$  Hz, 1H), 3.38 (s, 3H);  $^{13}\text{C NMR}$  ( $\text{CDCl}_3$ , 125 MHz):  $\delta$  170.0, 169.0, 142.7, 138.3, 131.6, 130.8, 130.2, 130.0, 129.6, 129.4, 128.5, 122.6, 56.4 (quintet,  $^1J_{\text{CD}} = 22.1$  Hz), 34.9; HRMS(EI) calcd for  $\text{C}_{16}\text{H}_{12}\text{ClN}_2\text{O}$  ( $\text{M} + \text{H}$ )<sup>+</sup> 287.0915, found 287.0941 (+9.29 ppm, +2.6 mDa).

**Kinetic Studies.** Samples of *ax-d*<sub>1</sub>-**5d–g** were dissolved in  $\text{CDCl}_3$  or  $\text{DMSO-}d_6$  and heated to 55 °C (**5d,f**), 98 °C (**5e**), or 100 °C (**5g**), and the mole fraction of the *ax-d*<sub>1</sub>-conformer ( $X_A$ ) was determined by  $^1\text{H NMR}$  integration. Kinetic runs at 55 °C were performed with the sample continuously in the probe; the probe temperature was previously calibrated with reference to the signals of ethylene glycol. Kinetic runs at 98 and 100 °C were performed by placing the NMR tube in a heated water bath for the designated time and then removing the tube and placing it in an ice bath until NMR analysis could be performed. Equilibrations were followed for 4–5 half-lives, and plots of  $\ln[2X_A - 1]$  vs time gave linear plots with  $R^2 > 0.98$ , as illustrated in Figure 2 for **5d**. The slope of these plots corresponds to  $-k_{\text{equil}} = -2k_{\text{enant}}$  (Scheme 4). The raw data for **5d–g** and kinetic plots for **5e–g** are provided in the Supporting Information.

**Computational Methods.** All density functional theory calculations were performed using the B3LYP<sup>29,30</sup> functional and 6-31G\* basis set in Gaussian 03.<sup>21</sup> All structures were characterized by vibrational frequency analysis as minima (no imaginary frequencies) or transition structures (one imaginary frequency). For all enantiomerization transition structures, the vector associated with the imaginary frequency corresponded to an inversion of the benzodiazepine ring. Note that these enantiomerization transition structures are not  $C_s$ -symmetric and thus exist as a pair of (*M*)- and (*P*)-enantiomers.<sup>14</sup> Note that for *N*-isopropyl structures, all three possible conformations around the N1–*i*-Pr bond were used as starting geometries to ensure that the minimum energy equilibrium geometries and transition structures were located. Zero point energy corrections were calculated from vibrational frequencies scaled by 0.9826;<sup>31</sup> free energy corrections were calculated using the same scaling factor, at the temperature of the corresponding kinetic experiment. Implicit solvent corrections were calculated by means of PCM<sup>32,33</sup> single-point calculations in the solvent of the corresponding kinetic experiment: the default radii (UA0) and surface (SES) of Gaussian 03 were used for these calculations.

**Acknowledgment.** We thank the National Science Foundation (CHE-0750006) and the Department of Chemistry, Virginia Tech, for financial support of this work.

**Supporting Information Available:** Synthetic procedures and tabulations of analytical data for **5f,g** and their 3-deuterio isotopomers;  $^1\text{H}$  and  $^{13}\text{C}$  NMR spectra for all compounds disclosed in the paper; kinetic data and plots; energies, Cartesian coordinates, and selected bond and dihedral angles of calculated structures. This material is available free of charge via the Internet at <http://pubs.acs.org>.

(29) Becke, A. *J. Chem. Phys.* **1993**, *98*, 5648–5652.

(30) Lee, C. T.; Yang, W. T.; Parr, R. G. *Phys. Rev. B* **1988**, *37*, 785–789.

(31) Merrick, J. P.; Moran, D.; Radom, L. *J. Phys. Chem. A* **2007**, *111*, 11683–11700.

(32) Miertus, S.; Scrocco, E.; Tomasi, J. *Chem. Phys.* **1981**, *55*, 117–129.

(33) Tomasi, J.; Mennucci, B.; Cammi, R. *Chem. Rev.* **2005**, *105*, 2999–3093.